

Precise Predictions for $\mu^\pm e^- \rightarrow \mu^\pm e^-$ at the MUonE Experiment

Alan Price 

Jagiellonian University, ul. prof. Stanisława Łojasiewicza 11, 30-348 Kraków, Poland

E-mail: alan.price@uj.edu.pl

ABSTRACT: The proposed fixed-target experiment, MUonE, at CERN will aim to measure the hadronic contribution to the running of the QED coupling by analysing the scattering of muons on electrons. Here we present state-of-the-art predictions for the process $\mu^\pm e^- \rightarrow \mu^\pm e^-$, where for the first time an all-order resummation of soft and soft-collinear logarithms has been performed. Further, we match this resummation with the complete next-to-leading and the dominant next-to-next-to-leading higher-order corrections. We find that the resummation has a dominant effect in the signal region, while the systematic matching significantly reduces the perturbative uncertainty.

Contents

| | | |
|----------|---------------------|-----------|
| 1 | Introduction | 1 |
| 2 | Theory | 2 |
| 3 | Results | 6 |
| 4 | Conclusion | 12 |

Contents

1 Introduction

The primary goal of the proposed MUonE experiment [1] at CERN will be to measure the hadronic contribution to the electromagnetic coupling, $\Delta\alpha_{\text{had}}(t)$, from the elastic collisions of a high-intensity muon beam upon a fixed target to induce $\mu^\pm e^- \rightarrow \mu^\pm e^-$ scattering. Since the structure of this scattering process contains no resonance structures, like those present at low-energy e^+e^- machines, it creates an optimal experimental environment for the extraction of $\Delta\alpha_{\text{had}}(t)$ as proposed in [2, 3] in the space-like region. For this result to be competitive with previous measurements of $\Delta\alpha_{\text{had}}(t)$, such as ones from dispersion relations [4–8] or lattice calculations [9–20], the uncertainty of the measured differential cross-sections at MUonE will have to be of the order of 10 ppm. In addition to the extraction of $\Delta\alpha_{\text{had}}(t)$, the MUonE experiment will also be able to probe a range of exotic beyond the Standard Model (BSM) scenarios [21–31].

For decades there has existed a discrepancy between the theoretical [32] and experimental [33, 34] values of a_μ [35] leading to a plethora of studies [36] which probed the physical implications of such an anomaly. However, recently the Muon g-2 experiment [37] E989 at Fermilab, which has combined two results from data taken over the past few years with a previous result from the Brookhaven National Laboratory (BNL) experiment [38] to reach an unprecedented accuracy of 0.20 ppm, has resolved this long standing anomaly with the uncertainties of the theory predictions. While this anomaly has been resolved within the Standard Model (SM), there exists a tension between the measured HVP contribution which are of the level of $2.5\text{--}5\sigma$. In particular, there exists a strong discrepancy between the CMD-3 results [39] from all previous measurements, and the deviation was significantly large enough that in the recent update of SM predictions the CMD-3 value could not be included in the common average of data-driven estimates for α_μ^{HLO} . In addition, an accurate measurement of $\Delta\alpha_{\text{had}}(t)$ will be an important input for future e^+e^- colliders [40–44], in particular for luminosity measurements where the uncertainty on the HVP will need to be reduced [45, 46], for which a direct measurement of $\Delta\alpha_{\text{had}}(t)$ will be invaluable.

On the theoretical side, $\mu^\pm e^- \rightarrow \mu^\pm e^-$ scattering has been studied in the past [47–55] using various different approaches and recently substantial progress has been made in developing modern Monte-Carlo tools, such as McMule [56] and MESMER [53, 57, 58], to compute electron–muon scattering at fixed-order accuracy at next-to-leading (NLO) and next-to-next-to-leading (NNLO) order and in which a wealth of recent theory calculations [58–80] have been developed for. However, despite these advances in the fixed-order calculations, considerably less attention has been given to another essential component of high-precision predictions, the resummation of soft and collinear logarithms arising from the emission of multiple photons. Depending on the kinematics of the phase space, these logarithms can become large and jeopardize the reliability of the perturbative expansion. Indeed, it has already been shown in [53, 57, 70], that in the signal region, which corresponds to low scattering angle of the electron, the effects of infrared (IR) logarithms, associated with the emission of soft photons, becomes quite sizeable.

One framework in which we can resum and tame the effects of such large logarithms is based on the Yennie–Frautschi–Suura (YFS) theorem [81]. This theorem allows us to reorganizes the entire perturbative expansion in such a way that all logarithms associated with infrared divergences are resummed to infinite order, leaving a finite remainder that can be computed to a high precision. It is also highly suitable for event generation, where it not only provides an accurate cross-section prediction, but in addition can generate the complete multi-photon [82] phase space. The YFS theorem has been implemented in many event generators [83–88], where most have focused on specific processes or decays, while the first automation to arbitrary lepton scattering processes was presented in SHERPA [89, 90]. Recently, we have expanded this implementation in SHERPA to automatically include NLO_{EW} and NNLO_{EW} corrections [91]. It is this implementation that we will use in this paper to calculate precise theory predictions for the MUonE experiment, where will have resummed all soft logarithms to infinite order, and additionally will provide the matching to the full NLO corrections and we will in addition include the NNLO corrections, where the only approximation we use will be in the two-loop corrections, however the dominant IR contributions will be included. Alternatively, one could consider resumming the large logarithms using a parton shower method [92, 93], which may be explored in a future work.

2 Theory

In fig. 1, we show the impact that the HVP has to the $\mu^+ e^- \rightarrow \mu^+ e^-$ observables that will be measured at MUonE. We use a dedicated interface in SHERPA to the stand-alone Fortran library *hadr5x23* [8, 94–97] to provide numerical values of $\Delta\alpha_{\text{had}}(t)$. We see that the largest effect can be seen at low electron angle, θ_e , in particular below 5 mrad where the effect is of order 10^{-3} . In the right plot of fig. 1 we see how the contribution depends on the Mandelstam variable $t_{e^- e^-}$. The MUonE experiment will aim to extract $\Delta\alpha_{\text{had}}(t)$ from this shape in the differential distributions by using a template fit method [1]. Schematically,

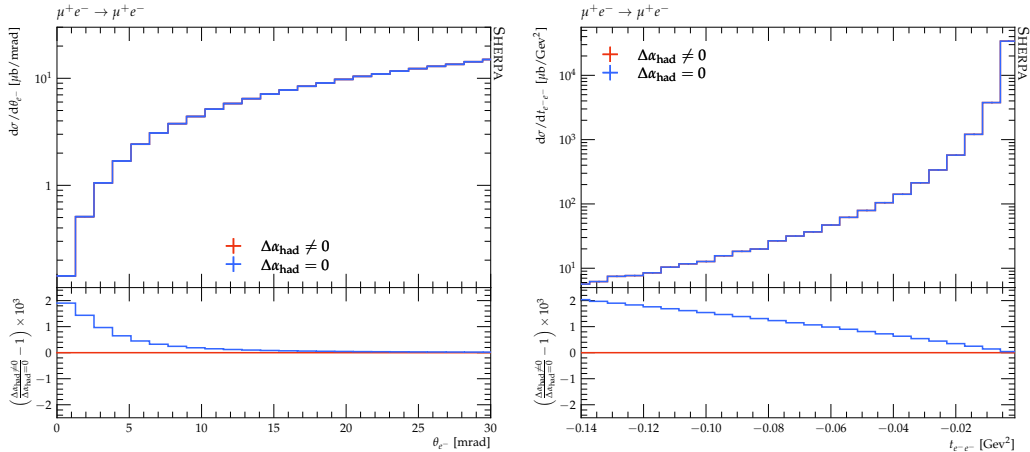


Figure 1. The impact of $\Delta\alpha_{\text{had}}(t)$ on electron observables at the MUonE experiment.

this can be thought as,

$$\frac{d\sigma^{\text{MUonE}}(t)}{d\sigma^{\text{MC}}(t) \big|_{\Delta\alpha_{\text{had}}(t)=0}} \approx 1 + 2\Delta\alpha_{\text{had}}(t) \quad (2.1)$$

where $d\sigma^{\text{MUonE}}(t)$ will be the measured differential distributions and $d\sigma^{\text{MC}}(t)$ are the MC predictions, where the numerical effects of $\Delta\alpha_{\text{had}}(t)$ are neglected. Therefore, it is crucial that any MC generator provides accurate predictions for the differential distributions, and it is this contribution that we will focus on in the rest of this work.

The YFS theorem states that the differential cross-section, encompassing all possible real and virtual photon emissions in an underlying Born process, is given by,

$$d\sigma^{(\infty)} = \sum_{n_\gamma=0}^{\infty} \frac{e^{Y(\Omega)}}{n_\gamma!} d\Phi_n \left[\prod_{i=1}^{n_\gamma} d\Phi_i^\gamma \tilde{S}(k_i) \Theta(k_i, \Omega) \right] \left(\tilde{\beta}_0(\Phi_n) + \sum_{j=1}^{n_\gamma} \frac{\tilde{\beta}_1(\Phi_{n+1})}{\tilde{S}(k_j)} + \sum_{\substack{j,k=1 \\ j < k}}^{n_\gamma} \frac{\tilde{\beta}_2(\Phi_{n+2})}{\tilde{S}(k_j) \tilde{S}(k_k)} + \dots \right). \quad (2.2)$$

Here, $d\Phi_n$ denotes the modified final state phase space element, the $d\Phi_i^\gamma$ are the phase space elements spanned by the n_γ real photon momenta k_i emitted off the leading order configuration. The infrared (IR) finite $\tilde{\beta}$ are the process-dependent terms in which we can include higher-order corrections. In the above expression, we have suppressed the indexing of unresolved emissions by introducing the following notation,

$$\tilde{\beta}_{n_R} = \sum_{n_V=0}^{\infty} \tilde{\beta}_{n_R}^{n_V+n_R}, \quad (2.3)$$

where n_R, n_V are the number of resolved and unresolved emissions under consideration. The NLO_{EW} corrections can be included by considering both the virtual, $\tilde{\beta}_0^1$ and real, $\tilde{\beta}_1^1$, corrections which can be calculated by,

$$\tilde{\beta}_0^1(\Phi_n) = \mathcal{V}(\Phi_n) - \sum_{ij} \mathcal{D}_{ij}(\Phi_{ij} \otimes \Phi_n), \quad (2.4)$$

$$\tilde{\beta}_1^1(\Phi_{n+1}) = \frac{1}{2(2\pi)^3} \mathcal{R}(\Phi_{n+1}) - \sum_{ij} \tilde{\mathcal{D}}_{ij}(\Phi_{ij} \otimes \Phi_k). \quad (2.5)$$

Here $\mathcal{R}(\Phi_{n+1})$ represents the squared amplitude which arises from all diagrams that can be constructed by considering one additional real photon to the born process and similarly $\mathcal{V}(\Phi_n)$ represents the complete virtual NLO corrections. The second terms in eqs. (2.4) and (2.5) are the corresponding subtraction terms which render the correction IR finite, which are automatically calculated in SHERPA [91]. At NNLO, we need to include additional corrections, namely,

$$\tilde{\beta}_1^2(\Phi_{n+1}) = \mathcal{R}\mathcal{V}(\Phi_{n+1}) - \sum_{ij} \mathcal{D}_{ij}^{(1)}(\Phi_{ij+1} \otimes \Phi_n), \quad (2.6)$$

$$\begin{aligned} \tilde{\beta}_2^2(\Phi_{n+2}) &= \mathcal{R}\mathcal{R}(\Phi_{n+2}) - \tilde{S}(k_1) \tilde{\beta}_1^1(\Phi_{n+1}; k_2) - \tilde{S}(k_2) \tilde{\beta}_1^1(\Phi_{n+1}; k_1) \\ &\quad - \tilde{S}(k_1) \tilde{S}(k_2) \tilde{\beta}_0^0(\Phi_n), \end{aligned} \quad (2.7)$$

$$\begin{aligned} \tilde{\beta}_0^2(\Phi_n) &= \mathcal{V}\mathcal{V}(\Phi_n) - \sum_{ij} \mathcal{D}_{ij}(\Phi_{ij} \otimes \Phi_n) \tilde{\beta}_0^1(\Phi_n) \\ &\quad - \frac{1}{2} \left(\sum_{ij} \mathcal{D}_{ij}(\Phi_{ij} \otimes \Phi_n) \right)^2 \tilde{\beta}_0^0(\Phi_n), \end{aligned} \quad (2.8)$$

where $\mathcal{R}\mathcal{V}(\Phi_{n+1})$ is the real-virtual, $\mathcal{R}\mathcal{R}(\Phi_{n+2})$ is the double real, and $\mathcal{V}\mathcal{V}(\Phi_n)$ is the double virtual corrections, and again each contribution has its own subtraction term. The explicit forms of the subtraction terms for each contribution can be found in [91]. Currently, there is no publicly available calculation of the two-loop contribution that suits our needs. In particular, we need a calculation that takes into account all mass terms explicitly such that the collinear divergences can be regulated. Although there has been some progress in the calculation of such amplitudes for other processes, such as Bhabha [63], the hierarchy of masses in our process remains a challenging bottleneck. We stress that when such a calculation becomes available for us, it can be easily incorporated into our framework. For now we shall only include the dominant IR contributions from the double-virtual while the sub-leading non-IR enhanced corrections are neglected, which is a similar approach as [57].

The tree-level amplitudes are obtained using one of SHERPA's internal automated matrix-element generators, either AMEGIC [98] or COMIX [99]. The one-loop corrections are computed through dedicated interfaces [100, 101] to external tools such as RECOLA [102] and OPENLOOPS [103] which in turn use tools such as COLLIER [104], CUTTOOLS [105] and ONELOOP [106] to help their numerical evaluations. We demonstrate in fig. 2 how the sub-

traction procedure successfully removes the IR-divergent contributions. In the upper row, we illustrate how the ϵ poles that encode the infrared divergences of the amplitudes in a loop cancel against the poles in the YFS subtraction term. For most events, this cancellation is accurate to 15 digits or more, which we consider sufficient for both the virtual and the real-virtual corrections. The bottom row shows the behaviour of the tree-level contributions for the real emissions coming from eqs. (2.5) and (2.7), normalised to the Born. On the left, we display the behaviour of eq. (2.5) in the limit where the photon energy becomes soft. This limit is especially relevant for MuonE, since in the signal region used for extracting $\Delta\alpha_{\text{had}}(t)$, the electron phasespace is constrained such that soft-photon radiation becomes dominant. Consequently, achieving precise predictions requires a matching procedure that remains numerically stable in the soft-emission limit, as confirmed by the lower-left panel of fig. 2. We observe that the contribution to eq. (2.5) becomes negligible as the photon energy approaches zero, reflecting the fact that the effects of such emissions are already incorporated in the resummation. In the bottom right of fig. 2 we examine the limiting behaviour of eq. (2.7). For such contributions, there are three limits of interest, namely the limit where one photon becomes soft and the other remains hard, and the limit where both photons become soft. In the former case, we expect the hard photon contribution will saturate the contribution while the soft photon contribution is removed by the subtraction term. In the case where both photons become soft, we expect the overall contribution to approach 0, which we see in our plot.

Before we discuss the full physical results of this paper, it is worthwhile examining the effect of our resummation in the signal region of the MUonE experiment. It is possible to undo the YFS resummation to investigate its effects, and this can be achieved by expanding eq. (2.2) and truncating it to a given fixed order within the MC. This truncated expression can then be used as an approximation of the fixed-order corrections where effects of resummation have been removed. And while the full resummed results will include multiple photon emission, the truncated approximation will only include a fixed number of photons. In fig. 3, we present a prediction where we truncate the YFS expansion at $\mathcal{O}(\alpha)$ and include both the leading-order (LO) and resummed predictions. At large scattering angles, there is little difference between the resummed and truncated predictions. However, in the signal region, $\theta_e \leq 5$, a significant difference emerges. Here, the photon emissions from the electron line are quite soft, leading to large logarithmic corrections that increase as we approach $\theta_e \rightarrow 0$. By enabling YFS, we can tame this divergent behaviour by resumming the problematic logarithms. While there's still a correction of approximately 50% compared to the LO predictions, we'll show in the next section that this is purely a perturbative uncertainty that can be systematically improved by including higher-order corrections. This indicates that the fixed-order expansion is unreliable in this region and to have physically sensible results for the MUonE experiment it will be mandatory to include resummation.

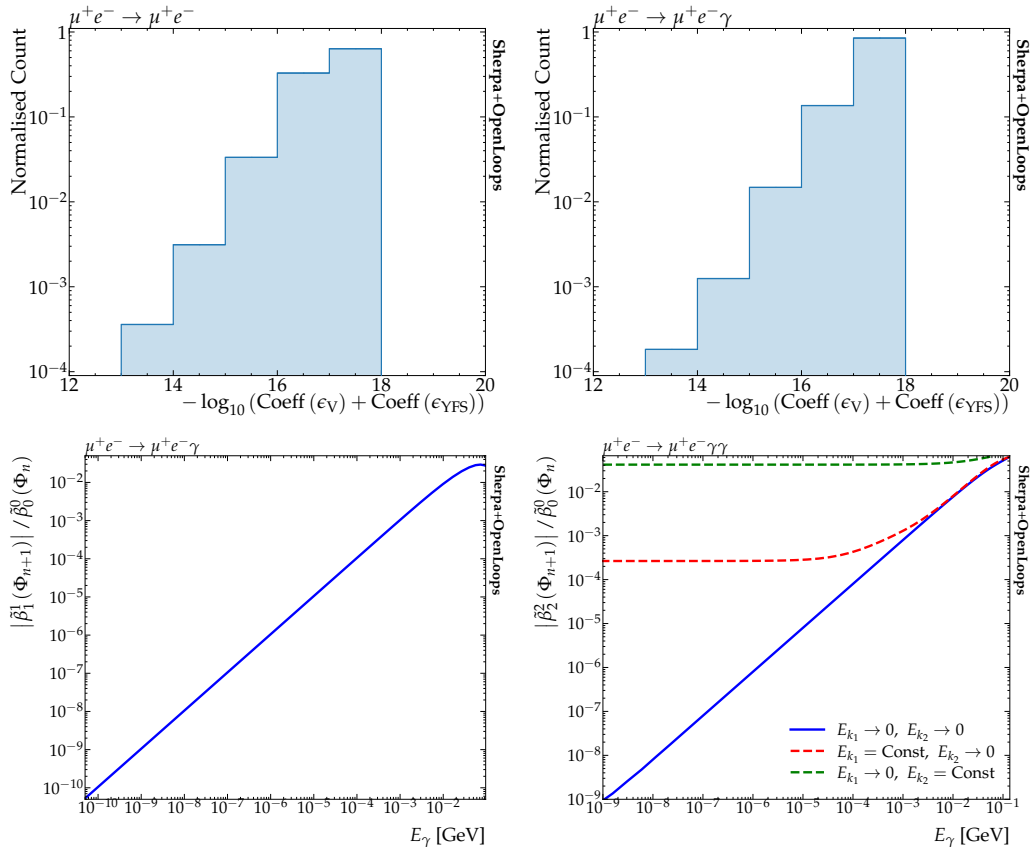


Figure 2. Top: The number of digits the pole cancellations are achieved to for both the virtual (left) and real-virtual (right) corrections in dimensional regularization. Bottom: The behaviour of the real (left) and double-real (right) corrections in the limit where photon momentum becomes ultra-soft.

3 Results

For real-world studies of $\mu^\pm e^- \rightarrow \mu^\pm e^-$ we will consider both the complete one-loop and real corrections in association with the full resummation of both ISR and FSR which will allow us to provide matched NLO_{EW} predictions. In addition, we will examine the effects of including the double real and real-virtual corrections, while the full two loop corrections are approximated using the YFS method similar to [57]. All leptons are treated as fully massive and the multiphoton phase space [90] will be treated completely analytically. Throughout this calculation, we employ the $\alpha(0)$ scheme where the input parameters are α , M_W , and M_Z and the explicit values can be found in table 1. We do not consider any of the background processes, which have been studied in great detail in [58, 107, 108]. We do note that in SHERPA it is possible to simulate $\mu^\pm e^- \rightarrow \mu^\pm e^- \ell \bar{\ell}$ within our YFS framework but as we identify this as a separate unique LO process we will not address it here but defer it to a future work. In the lab frame, we assume the muon beam is travelling in the positive

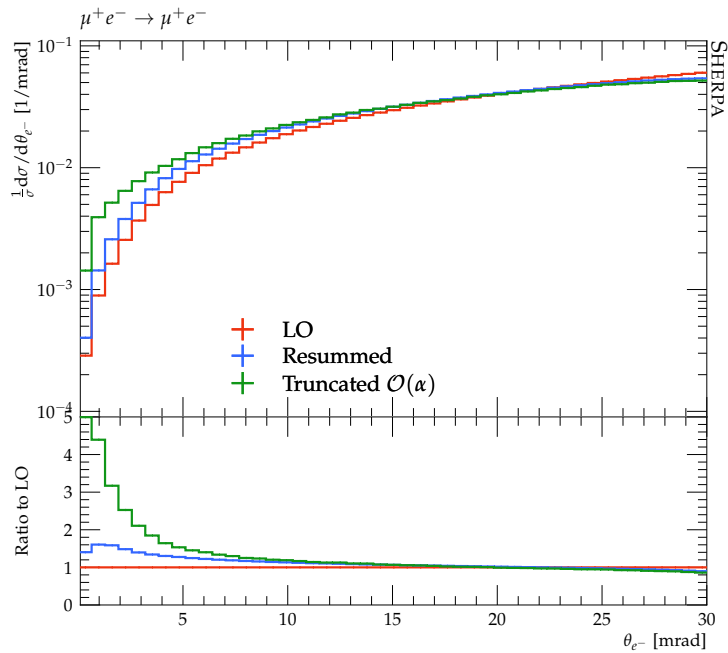


Figure 3. Leading-order, resummed, and truncated predictions for the electron’s scattering angle. The truncated expansion includes only the NLO fixed-order corrections.

| | Mass [GeV] | Width [GeV] |
|------------------|--------------|---------------|
| Z | 91.1876 | 2.4952 |
| W | 80.398 | 2.085 |
| e | 0.000511 | - |
| μ | 0.105 | - |
| $\alpha^{-1}(0)$ | 137.03599976 | |

Table 1. Electroweak input parameters in the $\alpha(0)$ scheme.

z-direction with an energy of 150 GeV ¹. We have implemented a dedicated fixed-target mode in SHERPA where the initial beams will be given as,

$$\begin{aligned}
 p_{\mu^\pm}^{\text{Lab}} &= (150, 0, 0, p_{\mu^\pm}^z) \\
 p_{e^-}^{\text{Lab}} &= (m_e, 0, 0, 0).
 \end{aligned}
 \tag{3.1}$$

We then boost the beams to the centre-of-mass frame, where we perform our calculation, and then finally boost back to lab frame where we analyse our events with the RIVET

¹While the actual beam will be 160 GeV, this value was chosen to align with previous studies by event generators. This has no effect on our conclusions.

package [109, 110]. For all our scenarios we follow a similar setup compared to previous fixed-order studies [57] and apply the following phasespace cuts in the lab frame,

$$\begin{aligned} E_{e^-} &> 1 \text{ GeV} \\ \theta_e, \theta_\mu &< 100 \text{ mrad.} \end{aligned} \quad (3.2)$$

and additionally we also include two separate cuts on the acoplanarity,

$$|\pi - |\Delta\phi_{\mu+e^-}|| \leq [3.5 \text{ mrad}, 0.4 \text{ rad}] \quad (3.3)$$

where the first cut follows from previous studies while the second is a more realistic experimental cut for the MUonE experiment [107, 111]. A strict cut, such as our first choice, will remove a significant amount of radiative events and enhance the number of elastic events. It is a useful cut for examine the impact of soft radiation which is not completely removed by such a cut.

We will consider three levels of correction, YFS_{LO} , YFS_{NLO} , and YFS_{nNLO} . The YFS_{LO} predictions will include the resummation of both the initial and final photon emissions, including interference effects, while the perturbative expansion will be truncated to LO only, which is simply the $\tilde{\beta}_0^0$ term. The YFS_{NLO} distributions include the same resummation, however the complete resolved and unresolved $\mathcal{O}(\alpha)$ corrections are included as described in eqs. (2.4) and (2.5). Finally, the YFS_{nNLO} predictions will additionally include the complete double real and real-virtual corrections, while we employ a YFS inspired approximation to the two-loop, where the dominant IR corrections have been resummed while the sub-leading non-IR enhancements have been included in the leading-log approximation [112]. Due to the missing non-IR terms in the two-loop corrections we use a lower-case "n" to represent these corrections. All one-loop amplitudes which appear in $\tilde{\beta}_0^1$ and $\tilde{\beta}_1^2$ will be calculated using SHERPA's interface to OPENLOOPS to calculate the virtual corrections. The remaining tree-level amplitudes, subtraction terms, and phasespace integrations are handled automatically by SHERPA. Similarly to [55] we find the weak contributions have small effect and neglect them in the remainder of this work.

We will calculate the size of our corrections by taking the difference with the next lowest order prediction,

$$\Delta\text{YFS}_i = \left(\frac{\text{YFS}_i}{\text{YFS}_{i-1}} - 1 \right) \times 100 \quad i \in (\text{LO}, \text{NLO}, \text{nNLO}) \quad (3.4)$$

and for $\Delta\text{YFS}_{\text{LO}}$ we take the reference to be the Born-level prediction without any resummation effects.

In fig. 4, we show these three predictions for the polar angle of the electron in the lab frame. In the scenario without any acoplanarity cut, we see that $\Delta\text{YFS}_{\text{LO}}$ at large angles has a negative impact of $\approx 10\%$, which as we approach $\theta_e = 0$ changes signs and grows to be of the order of 60%. It is interesting to note that this behaviour replicates the NLO predictions of the fixed-order tools, particularly in the large angle region. This means that YFS_{LO} already captures the dominant effects of the NLO fixed-order predictions, even

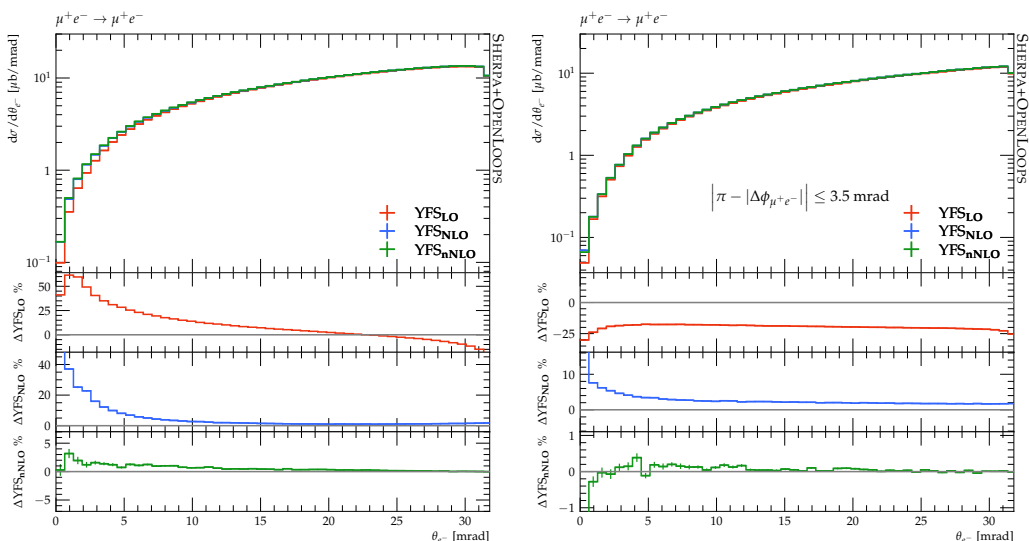


Figure 4. Electron polar angle distribution for different sign scenario for YFS_{LO} (red), YFS_{NLO} (blue), and YFS_{nNLO} (green).

before we include our matching. When the acoplanarity cut has been included we see that the correction remains fairly flat around 25%, we attribute the flatness to the reduction of hard photon radiation, however the YFS will induce a change in the total cross-section hence the overall normalization. For the $\Delta\text{YFS}_{\text{NLO}}$ contributions, we see that the correction becomes flat in the large angle region, around 2%, while as we approach the signal region it grows to around 40%, but with a gentler slope compared to $\Delta\text{YFS}_{\text{LO}}$. We attribute the size of this correction to the collinear enhanced logarithms which appear for the first time at this order. We see a similar correction in the hard region when employing the acoplanarity cut, while in the signal region we see a factor 2 reduction when compared to the setup without this cut. This implies that a large source of our uncertainty in this region can be attributed to the hard and collinear photon emissions. For the YFS_{nNLO} contributions we see quite an improvement in the large angle region. Here the uncertainty due to missing higher order corrections drops to $\approx 0.01\%$, which is a similar precision of the LEP era YFS generators [84, 113].

In fig. 5, we present the electron angular distributions for the same-sign scenario. In the first scenario, we see a very similar results as in the $\mu^+e^- \rightarrow \mu^+e^-$ case. We note that when the acoplanarity cut is applied we see a smaller uncertainty for YFS_{NLO} case.

Figure 6 shows the $t_{e^-e^-}$ distribution for $\mu^+e^- \rightarrow \mu^+e^-$. For YFS_{LO} we again see a large correction in the signal region, while in the small $|t_{e^-e^-}|$ region we observe a sign change. The shape and the magnitude of $\Delta\text{YFS}_{\text{LO}}$ is similar to that observed by the fixed-order predictions, particularly at low $|t_{e^-e^-}|$, while for large $|t_{e^-e^-}|$ we have slightly smaller correction. For YFS_{NLO} we see that our correction becomes relatively flat in the majority of the region while as we approach $t_{e^-e^-} = -0.14 \text{ GeV}^2$ the effect grows to 10%. Finally, for YFS_{nNLO} we see the corrections remain stable and bring our overall correction down to

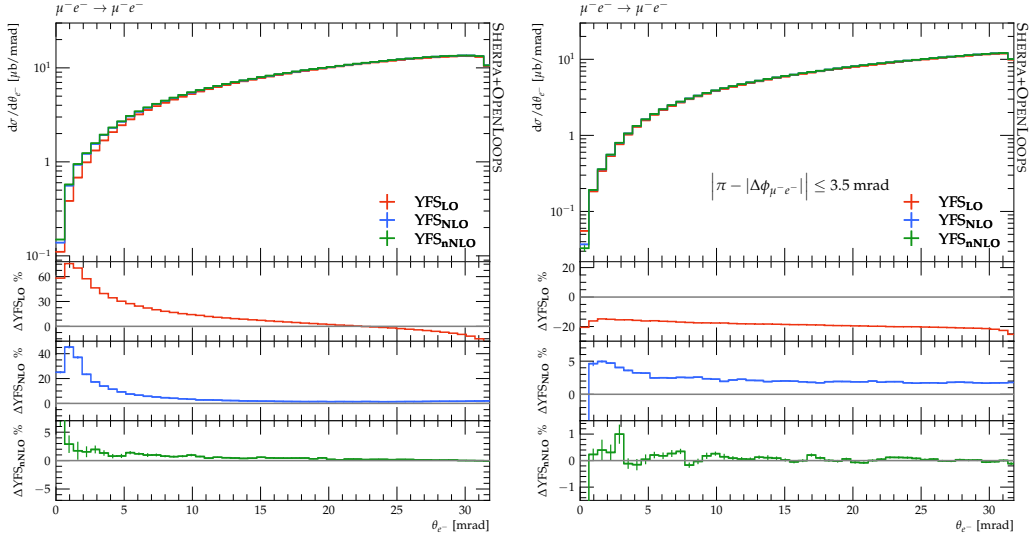


Figure 5. Electron polar angle distribution for same sign scenario for YFS_{LO} (red), YFS_{NLO} (blue), and YFS_{nNLO} (green).

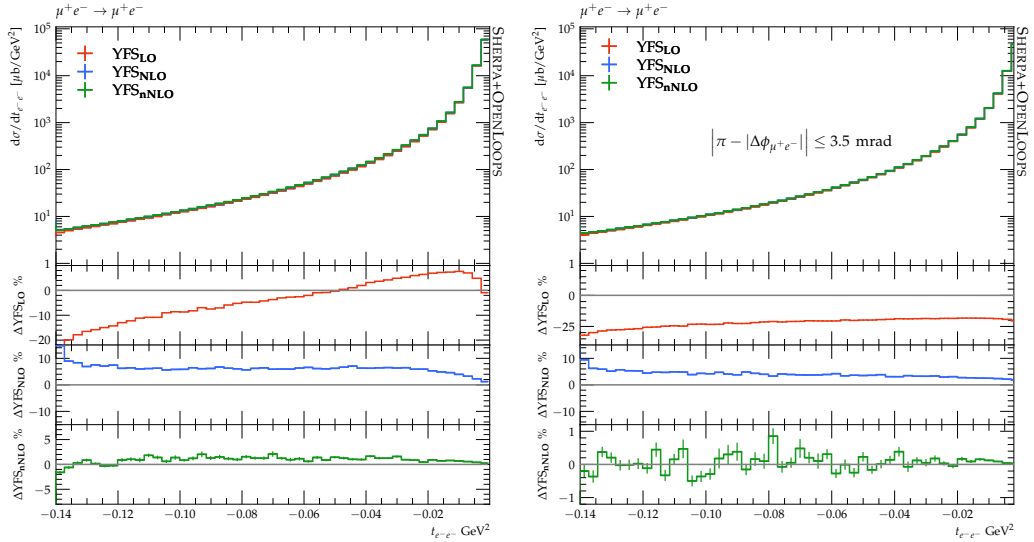


Figure 6. t_{e-e-} distribution for different sign scenario for YFS_{LO} (red), YFS_{NLO} (blue), and YFS_{nNLO} (green).

the percent level. When the additional acoplanarity cut is applied we see that the $\Delta\text{YFS}_{\text{LO}}$ is relatively flat around -25% , again reflecting the fact that we have removed a significant amount of the hard ISR/FSR radiation. The $\Delta\text{YFS}_{\text{NLO}}$ is slightly improved over the case without the acoplanarity cut. For YFS_{nNLO} the corrections are at the per-mille level which is approaching the 10 ppm level, which is roughly factor 10 improvement over the scenario without an acoplanarity cut. This reflects again that our uncertainty is mostly due to the hard radiation which we have removed with the additional cut. In figs. 7 and 8, we examine

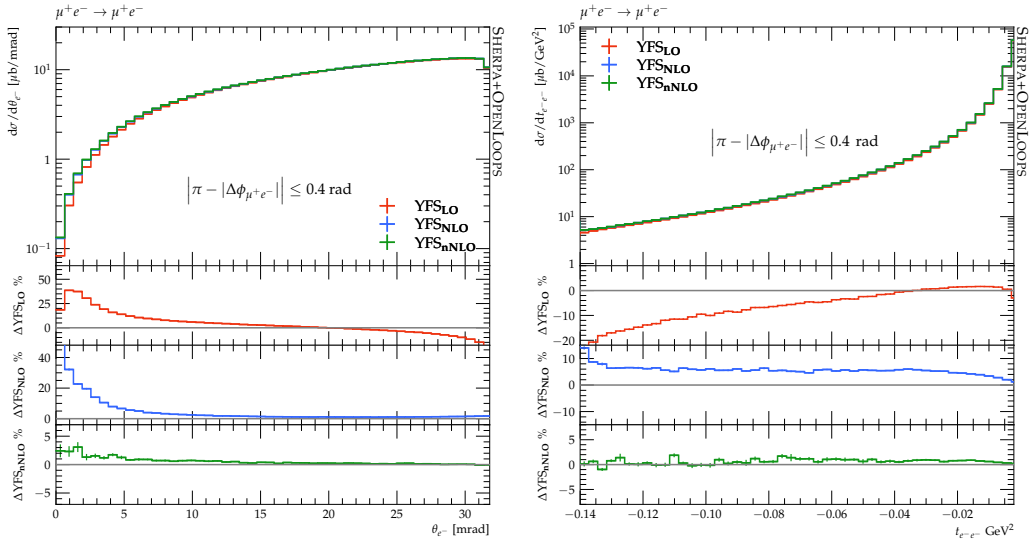


Figure 7. Electron polar angle (left) and $t_{e^-e^-}$ (right) distributions for different sign scenarios, including a realistic acoplanarity cut.

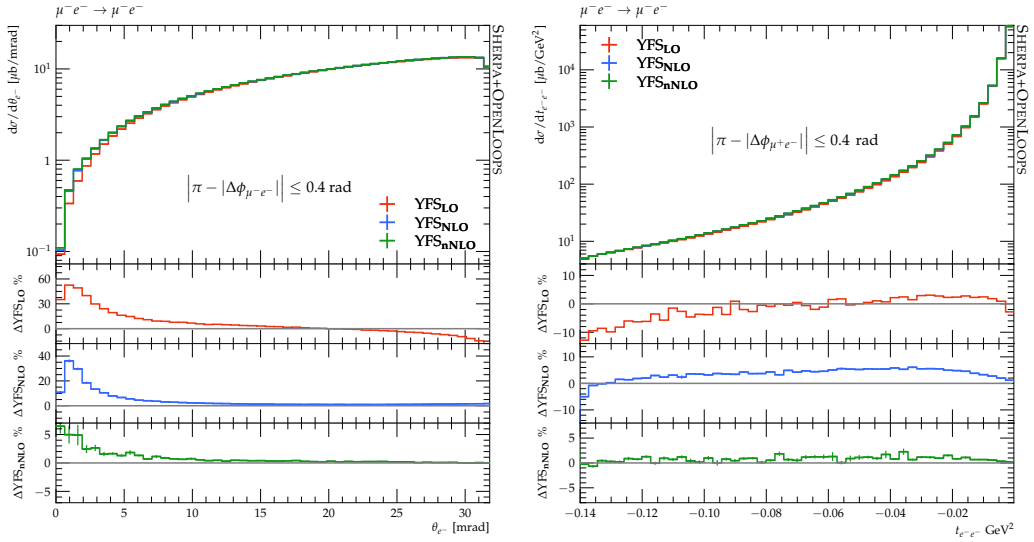


Figure 8. Electron polar angle (left) and $t_{e^-e^-}$ (right) distributions for different sign scenarios, including a realistic acoplanarity cut.

the effects of a more realistic acoplanarity cut of 0.4 rad. We see that $\Delta\text{YFS}_{\text{LO}}$ becomes smaller in the signal region, as the inclusion of this cut suppresses some of the photon radiation generated, which reduces the impact of YFS_{LO} . For the higher-order corrections, the inclusion of this cut has little effect on our uncertainty estimates. This simply reflects the fact that the effect of the cut is present at each order and is largely cancelled in the ratio of eq. (3.4). While we do not have the complete NNLO correction we tentatively approximate the size of uncertainty by considering the scaling between successive orders

as an approximation of missing higher-orders. We can safely do this as we know the YFS series, eq. (2.2), is well-behaved and free of singularities. In the signal region we can take the approximate missing third order corrections to be of the order $\frac{\Delta\text{YFS}_{\text{nNLO}}}{\Delta\text{YFS}_{\text{NLO}}} \times \Delta\text{YFS}_{\text{nNLO}}$. With this we estimate that our uncertainty in signal region for the first setup is of the order 0.2% while with the addition of the acoplanarity cut this gets further reduced to 0.001% which is within the 10 ppm accuracy needed by MUonE. However, we should stress that this uncertainty arises from missing higher-order corrections and may not reflect the true theoretical uncertainty. In particular, we will need to compare against other approaches, such as collinear-based parton showers, and carefully examine any differences with our YFS approach, incorporating these into our error budget before we can give a conclusive estimate for the complete theoretical uncertainty.

4 Conclusion

In this paper, we studied the effect of QED resummation on $\mu^\pm e^- \rightarrow \mu^\pm e^-$ process at the proposed MUonE experiment. We found that the effect of this resummation are sizeable particularly in the signal region. From this, we conclude that at the MUonE experiment, one cannot neglect the effects of resummation and it will be mandatory to include if we reach the 10 ppm precision needed to extract an accurate measurement of $\Delta\alpha_{\text{Had}}$. In particular we have resolved the instabilities seen at $\theta_e < 5$ mrad, which had plagued the fixed-order predictions. We have shown how one can match the YFS resummation to the complete NLO and NNLO, where the only approximation we have taken is in regards to the two-loop corrections. We find that in order-by-order comparisons the uncertainty in our calculation improves, from $\approx 50\%$ for the YFS_{LO} down to $\approx 5\%$ for YFS_{nNLO} in the inclusive scenario. When apply the additional cut on the acoplanarity these uncertainties enter the per-mil level, approaching the 10 ppm level needed by MUonE experiment. While this acoplanarity cut may be too harsh for the experimental environment, as it may remove too many non-elastic scattering events, it implies that selectively removing hard radiation events may be one avenue to reaching the precision needed. We estimate that our theoretical uncertainties are at a level of 0.2%, which is still insufficient for the MUonE experiment, even prior to accounting for method-dependent contributions. It is possible that the inclusion of the N^3LO corrections will allow us to reach the precision needs of the MUonE experiment. We believe that it will be feasible to include a subset of these corrections, namely the tree-level and one-loop corrections which will arise at N^3LO , which we know how to include in the YFS formalism. However, the two-loop and three-loop contributions pose a significant challenge, and alternative approaches may need to be explored. Another avenue to consider is the potential for combining our YFS-based resummation with a collinear approach. While combining YFS with a full parton-shower presents many difficulties, we might be able to include some higher-order effects arising from the collinear splitting of photons into lepton pairs, as described in [93].

Acknowledgements

A.P would like to thank Fred Jegerlehner who reignited my interest in this project and Wieslaw Płaczek for comments on the manuscript and for many discussions on the treatment of YFS form factor. We would also like to thank the MESMER collaboration for multiple conversations and to Carlo Carloni Calame for reading the draft manuscript. The work of A.P. is supported by grant No. 2023/50/A/ST2/00224 of the National Science Centre (NCN), Poland. We gratefully acknowledge Polish high-performance computing infrastructure PLGrid (HPC Center: ACK Cyfronet AGH) for providing computer facilities and support within computational grant no. PLG/2025/018139.

References

- [1] MUONE collaboration, *Letter of Intent: the MUonE project*, Tech. Rep. CERN-SPSC-2019-026, SPSC-I-252, CERN, Geneva (Jun, 2019).
- [2] C.M. Carloni Calame, M. Passera, L. Trentadue and G. Venanzoni, *A new approach to evaluate the leading hadronic corrections to the muon $g-2$* , *Phys. Lett. B* **746** (2015) 325 [[1504.02228](#)].
- [3] G. Abbiendi et al., *Measuring the leading hadronic contribution to the muon $g-2$ via μe scattering*, *Eur. Phys. J. C* **77** (2017) 139 [[1609.08987](#)].
- [4] R. Aliberti et al., *The anomalous magnetic moment of the muon in the Standard Model: an update*, *Phys. Rept.* **1143** (2025) 1 [[2505.21476](#)].
- [5] M. Davier, A. Hoecker, B. Malaescu and Z. Zhang, *A new evaluation of the hadronic vacuum polarisation contributions to the muon anomalous magnetic moment and to $\alpha(m_Z^2)$* , *Eur. Phys. J. C* **80** (2020) 241 [[1908.00921](#)].
- [6] A. Keshavarzi, D. Nomura and T. Teubner, *Muon $g - 2$ and $\alpha(M_Z^2)$: a new data-based analysis*, *Phys. Rev. D* **97** (2018) 114025 [[1802.02995](#)].
- [7] F. Jegerlehner, *The Muon $g-2$ in Progress*, *Acta Phys. Polon. B* **49** (2018) 1157 [[1804.07409](#)].
- [8] F. Jegerlehner, *Precision measurements of $\sigma(\text{hadronic})$ for $\alpha(\text{eff})(E)$ at ILC energies and $(g-2)(\mu)$* , *Nucl. Phys. B Proc. Suppl.* **162** (2006) 22 [[hep-ph/0608329](#)].
- [9] M. Della Morte, A. Francis, V. Gülpers, G. Herdoíza, G. von Hippel, H. Horch et al., *The hadronic vacuum polarization contribution to the muon $g - 2$ from lattice QCD*, *JHEP* **10** (2017) 020 [[1705.01775](#)].
- [10] FERMILAB LATTICE, LATTICE-HPQCD, MILC collaboration, *Strong-Isospin-Breaking Correction to the Muon Anomalous Magnetic Moment from Lattice QCD at the Physical Point*, *Phys. Rev. Lett.* **120** (2018) 152001 [[1710.11212](#)].
- [11] BUDAPEST-MARSEILLE-WUPPERTAL collaboration, *Hadronic vacuum polarization contribution to the anomalous magnetic moments of leptons from first principles*, *Phys. Rev. Lett.* **121** (2018) 022002 [[1711.04980](#)].
- [12] H.B. Meyer and H. Wittig, *Lattice QCD and the anomalous magnetic moment of the muon*, *Prog. Part. Nucl. Phys.* **104** (2019) 46 [[1807.09370](#)].

- [13] RBC, UKQCD collaboration, *Calculation of the hadronic vacuum polarization contribution to the muon anomalous magnetic moment*, *Phys. Rev. Lett.* **121** (2018) 022003 [[1801.07224](#)].
- [14] D. Giusti, F. Sanfilippo and S. Simula, *Light-quark contribution to the leading hadronic vacuum polarization term of the muon $g - 2$ from twisted-mass fermions*, *Phys. Rev. D* **98** (2018) 114504 [[1808.00887](#)].
- [15] D. Giusti, V. Lubicz, G. Martinelli, F. Sanfilippo and S. Simula, *Electromagnetic and strong isospin-breaking corrections to the muon $g - 2$ from Lattice QCD+QED*, *Phys. Rev. D* **99** (2019) 114502 [[1901.10462](#)].
- [16] D. Giusti and S. Simula, *Lepton anomalous magnetic moments in Lattice QCD+QED*, *PoS LATTICE2019* (2019) 104 [[1910.03874](#)].
- [17] PACS collaboration, *Hadronic vacuum polarization contribution to the muon $g - 2$ with $2+1$ flavor lattice QCD on a larger than $(10 \text{ fm})^4$ lattice at the physical point*, *Phys. Rev. D* **100** (2019) 034517 [[1902.00885](#)].
- [18] FERMILAB LATTICE, LATTICE-HPQCD, MILC collaboration, *Hadronic-vacuum-polarization contribution to the muon's anomalous magnetic moment from four-flavor lattice QCD*, *Phys. Rev. D* **101** (2020) 034512 [[1902.04223](#)].
- [19] A. Gérardin, M. Cè, G. von Hippel, B. Hörz, H.B. Meyer, D. Mohler et al., *The leading hadronic contribution to $(g - 2)_\mu$ from lattice QCD with $N_f = 2 + 1$ flavours of $O(a)$ improved Wilson quarks*, *Phys. Rev. D* **100** (2019) 014510 [[1904.03120](#)].
- [20] C. Aubin, T. Blum, C. Tu, M. Golterman, C. Jung and S. Peris, *Light quark vacuum polarization at the physical point and contribution to the muon $g - 2$* , *Phys. Rev. D* **101** (2020) 014503 [[1905.09307](#)].
- [21] P.S.B. Dev, W. Rodejohann, X.-J. Xu and Y. Zhang, *MUonE sensitivity to new physics explanations of the muon anomalous magnetic moment*, *JHEP* **05** (2020) 053 [[2002.04822](#)].
- [22] Z. Wang et al., *Search for light Dark Sectors with GeV Muon Beams*, [2511.08950](#).
- [23] D. Rocha and I.R. Wang, *Filling the Gap: Hunting for Vector Bosons at the MUonE Experiment with Displaced Decay Signature*, [2511.03222](#).
- [24] G. Krnjaic, D. Rocha and I.R. Wang, *Discovering Dark Matter with the MUonE Experiment*, *Phys. Rev. Lett.* **134** (2025) 161801 [[2409.00170](#)].
- [25] B. Barman, A. Das and S. Mandal, *Dark matter-electron scattering and freeze-in scenarios in the light of Z' mediation*, *Phys. Rev. D* **110** (2024) 055029 [[2407.00969](#)].
- [26] K. Asai, A. Das, J. Li, T. Nomura and O. Seto, *Probing for chiral Z' gauge boson through scattering measurement experiments*, *Phys. Rev. D* **109** (2024) 075026 [[2307.09737](#)].
- [27] H. Sieber, D.V. Kirpichnikov, I.V. Voronchikhin, P. Crivelli, S.N. Gninenko, M.M. Kirsanov et al., *Probing hidden sectors with a muon beam: Implication of spin-0 dark matter mediators for the muon $(g-2)$ anomaly and the validity of the Weiszäcker-Williams approach*, *Phys. Rev. D* **108** (2023) 056018 [[2305.09015](#)].
- [28] O. Atkinson, M. Black, C. Englert, A. Lenz and A. Rusov, *MUonE, muon $g-2$ and electroweak precision constraints within 2HDMs*, *Phys. Rev. D* **106** (2022) 115031 [[2207.02789](#)].

- [29] G. Grilli di Cortona and E. Nardi, *Probing light mediators at the MUonE experiment*, *Phys. Rev. D* **105** (2022) L111701 [2204.04227].
- [30] I. Galon, D. Shih and I.R. Wang, *Dark photons and displaced vertices at the MUonE experiment*, *Phys. Rev. D* **107** (2023) 095003 [2202.08843].
- [31] A. Masiero, P. Paradisi and M. Passera, *New physics at the MUonE experiment at CERN*, *Phys. Rev. D* **102** (2020) 075013 [2002.05418].
- [32] T. Aoyama et al., *The anomalous magnetic moment of the muon in the Standard Model*, *Phys. Rept.* **887** (2020) 1 [2006.04822].
- [33] MUON G-2 collaboration, *Measurement of the Positive Muon Anomalous Magnetic Moment to 0.46 ppm*, *Phys. Rev. Lett.* **126** (2021) 141801 [2104.03281].
- [34] MUON G-2 collaboration, *Measurement of the Positive Muon Anomalous Magnetic Moment to 0.20 ppm*, *Phys. Rev. Lett.* **131** (2023) 161802 [2308.06230].
- [35] F. Jegerlehner and A. Nyffeler, *The Muon $g-2$* , *Phys. Rept.* **477** (2009) 1 [0902.3360].
- [36] P. Athron, K. Möhling, D. Stöckinger and H. Stöckinger-Kim, *The Muon Magnetic Moment and Physics Beyond the Standard Model*, **2507.09289**.
- [37] MUON G-2 collaboration, *Muon ($g-2$) Technical Design Report*, **1501.06858**.
- [38] MUON G-2 collaboration, *Final Report of the Muon E821 Anomalous Magnetic Moment Measurement at BNL*, *Phys. Rev. D* **73** (2006) 072003 [hep-ex/0602035].
- [39] CMD-3 collaboration, *Measurement of the $e+e-\rightarrow\pi+\pi-$ cross section from threshold to 1.2 GeV with the CMD-3 detector*, *Phys. Rev. D* **109** (2024) 112002 [2302.08834].
- [40] ILC collaboration, H. Baer et al., eds., *The International Linear Collider Technical Design Report - Volume 2: Physics*, **1306.6352**.
- [41] M. Aicheler, P. Burrows, M. Draper, T. Garvey, P. Lebrun, K. Peach et al., eds., *A Multi-TeV Linear Collider Based on CLIC Technology: CLIC Conceptual Design Report*, .
- [42] FCC collaboration, *FCC-ee: The Lepton Collider: Future Circular Collider Conceptual Design Report Volume 2*, *Eur. Phys. J. ST* **228** (2019) 261.
- [43] CEPC STUDY GROUP collaboration, *CEPC Conceptual Design Report: Volume 2 - Physics & Detector*, **1811.10545**.
- [44] C. Vernieri et al., *Strategy for Understanding the Higgs Physics: The Cool Copper Collider*, *JINST* **18** (2023) P07053 [2203.07646].
- [45] S. Jadach, W. Płaczek, M. Skrzypek, B.F.L. Ward and S.A. Yost, *The path to 0.01% theoretical luminosity precision for the FCC-ee*, *Phys. Lett. B* **790** (2019) 314 [1812.01004].
- [46] F. Jegerlehner, $\alpha_{QED,eff}(s)$ for precision physics at the FCC-ee/ILC, *CERN Yellow Reports: Monographs* **3** (2020) 9.
- [47] A. Nikishov, *Radiative corrections to the scattering of μ mesons on electrons*, *Sov.Phys.JETP* **12** (1961) 529.
- [48] K. Eriksson, *Radiative corrections to muon-electron scattering*, *Nuovo Cim.* **19** (1961) 1029.
- [49] G.R. K.E. Eriksson, B. Larsson, *Radiative corrections to muon-electron scattering*, *Nuovo Cim.* **30** (1963) 1434.

- [50] P. Van Nieuwenhuizen, *Muon-electron scattering cross-section to order alpha-to-the-third*, *Nucl. Phys. B* **28** (1971) 429.
- [51] T.V. Kukhto, N.M. Shumeiko and S.I. Timoshin, *Radiative Corrections in Polarized Electron Muon Elastic Scattering*, *J. Phys. G* **13** (1987) 725.
- [52] D.Y. Bardin and L. Kalinovskaya, *QED corrections for polarized elastic muon e scattering*, [hep-ph/9712310](#).
- [53] M. Alacevich, C.M. Carloni Calame, M. Chiesa, G. Montagna, O. Nicrosini and F. Piccinini, *Muon-electron scattering at NLO*, *JHEP* **02** (2019) 155 [[1811.06743](#)].
- [54] T. Engel, A. Signer and Y. Ulrich, *A subtraction scheme for massive QED*, *JHEP* **01** (2020) 085 [[1909.10244](#)].
- [55] C.M. Carloni Calame, M. Chiesa, G. Montagna, O. Nicrosini and F. Piccinini, *Muon-electron scattering at next-to-leading order accuracy*, *EPJ Web Conf.* **212** (2019) 05002.
- [56] P. Banerjee, T. Engel, A. Signer and Y. Ulrich, *QED at NNLO with McMule*, *SciPost Phys.* **9** (2020) 027 [[2007.01654](#)].
- [57] C.M. Carloni Calame, M. Chiesa, S.M. Hasan, G. Montagna, O. Nicrosini and F. Piccinini, *Towards muon-electron scattering at NNLO*, *JHEP* **11** (2020) 028 [[2007.01586](#)].
- [58] E. Budassi, C.M. Carloni Calame, M. Chiesa, C.L. Del Pio, S.M. Hasan, G. Montagna et al., *NNLO virtual and real leptonic corrections to muon-electron scattering*, *JHEP* **11** (2021) 098 [[2109.14606](#)].
- [59] P. Banerjee et al., *Theory for muon-electron scattering @ 10 ppm: A report of the MUonE theory initiative*, *Eur. Phys. J. C* **80** (2020) 591 [[2004.13663](#)].
- [60] P. Mastrolia, M. Passera, A. Primo and U. Schubert, *Master integrals for the NNLO virtual corrections to μe scattering in QED: the planar graphs*, *JHEP* **11** (2017) 198 [[1709.07435](#)].
- [61] S. Di Vita, S. Laporta, P. Mastrolia, A. Primo and U. Schubert, *Master integrals for the NNLO virtual corrections to μe scattering in QED: the non-planar graphs*, *JHEP* **09** (2018) 016 [[1806.08241](#)].
- [62] M. Fael, *Hadronic corrections to μ -e scattering at NNLO with space-like data*, *JHEP* **02** (2019) 027 [[1808.08233](#)].
- [63] M. Delto, C. Duhr, L. Tancredi and Y.J. Zhu, *Two-Loop QED Corrections to the Scattering of Four Massive Leptons*, *Phys. Rev. Lett.* **132** (2024) 231904 [[2311.06385](#)].
- [64] S. Badger, J. Kryś, R. Moodie and S. Zoia, *Lepton-pair scattering with an off-shell and an on-shell photon at two loops in massless QED*, *JHEP* **11** (2023) 041 [[2307.03098](#)].
- [65] M. Fael and M. Passera, *Muon-Electron Scattering at Next-To-Next-To-Leading Order: The Hadronic Corrections*, *Phys. Rev. Lett.* **122** (2019) 192001 [[1901.03106](#)].
- [66] T. Ahmed, G. Crisanti, F. Gasparotto, S.M. Hasan and P. Mastrolia, *Two-loop vertices with vacuum polarization insertion*, *JHEP* **01** (2024) 010 [[2308.05028](#)].
- [67] M. Fael, F. Lange, K. Schönwald and M. Steinhauser, *Massive Vector Form Factors to Three Loops*, *Phys. Rev. Lett.* **128** (2022) 172003 [[2202.05276](#)].
- [68] P. Mastrolia and E. Remiddi, *Two loop form-factors in QED*, *Nucl. Phys. B* **664** (2003) 341 [[hep-ph/0302162](#)].

- [69] M. Fael, F. Lange, K. Schönwald and M. Steinhauser, *Singlet and nonsinglet three-loop massive form factors*, *Phys. Rev. D* **106** (2022) 034029 [[2207.00027](#)].
- [70] A. Broggio et al., *Muon-electron scattering at NNLO*, *JHEP* **01** (2023) 112 [[2212.06481](#)].
- [71] R. Plestid and M.B. Wise, *Atomic binding corrections for high-energy fixed target experiments*, *Phys. Rev. D* **110** (2024) 056032 [[2403.12184](#)].
- [72] R. Bonciani et al., *Two-Loop Four-Fermion Scattering Amplitude in QED*, *Phys. Rev. Lett.* **128** (2022) 022002 [[2106.13179](#)].
- [73] T. Dave and W.J. Torres Bobadilla, *Helicity amplitudes in massless QED to higher orders in the dimensional regulator*, *Phys. Rev. D* **111** (2025) 036024 [[2411.07063](#)].
- [74] R. Plestid and M.B. Wise, *Final state interactions for high energy scattering off atomic electrons*, *Phys. Rev. D* **110** (2024) 113007 [[2407.21752](#)].
- [75] T. Engel, *The LBK theorem to all orders*, *JHEP* **07** (2023) 177 [[2304.11689](#)].
- [76] T. Engel, *Multiple soft-photon emission at next-to-leading power to all orders*, *JHEP* **03** (2024) 004 [[2311.17612](#)].
- [77] MUONE collaboration, *Theory for the MUonE experiment*, *PoS EPS-HEP2023* (2024) 307 [[2401.06491](#)].
- [78] E. Balzani, S. Laporta and M. Passera, *Hadronic vacuum polarization contributions to the muon $g-2$ in the space-like region*, *Phys. Lett. B* **834** (2022) 137462 [[2112.05704](#)].
- [79] J. Ronca, *NNLO QED contribution to the $\mu e \rightarrow \mu e$ elastic scattering*, *EPJ Web Conf.* **234** (2020) 01015 [[1912.05397](#)].
- [80] T. Engel, C. Gnendiger, A. Signer and Y. Ulrich, *Small-mass effects in heavy-to-light form factors*, *JHEP* **02** (2019) 118 [[1811.06461](#)].
- [81] D.R. Yennie, S.C. Frautschi and H. Suura, *The infrared divergence phenomena and high-energy processes*, *Annals Phys.* **13** (1961) 379.
- [82] S. Jadach and B.F.L. Ward, *Yfs2: The Second Order Monte Carlo for Fermion Pair Production at LEP / SLC With the Initial State Radiation of Two Hard and Multiple Soft Photons*, *Comput. Phys. Commun.* **56** (1990) 351.
- [83] S. Jadach, W. Placzek, E. Richter-Was, B.F.L. Ward and Z. Was, *Upgrade of the Monte Carlo program BHLUMI for Bhabha scattering at low angles to version 4.04*, *Comput. Phys. Commun.* **102** (1997) 229.
- [84] S. Jadach, W. Placzek and B.F.L. Ward, *BHWIDE 1.00: $O(\alpha)$ YFS exponentiated Monte Carlo for Bhabha scattering at wide angles for LEP-1 / SLC and LEP-2*, *Phys. Lett. B* **390** (1997) 298 [[hep-ph/9608412](#)].
- [85] M. Schonherr and F. Krauss, *Soft Photon Radiation in Particle Decays in SHERPA*, *JHEP* **12** (2008) 018 [[0810.5071](#)].
- [86] F. Krauss, J.M. Lindert, R. Linten and M. Schönherr, *Accurate simulation of W, Z and Higgs boson decays in Sherpa*, *Eur. Phys. J. C* **79** (2019) 143 [[1809.10650](#)].
- [87] K. Hamilton and P. Richardson, *Simulation of QED radiation in particle decays using the YFS formalism*, *JHEP* **07** (2006) 010 [[hep-ph/0603034](#)].
- [88] S. Jadach, W. Placzek, M. Skrzypek, B.F.L. Ward and Z. Was, *The Monte Carlo program KoralW version 1.51 and the concurrent Monte Carlo KoralW and YFSWW3 with all*

background graphs and first order corrections to W pair production, *Comput. Phys. Commun.* **140** (2001) 475 [[hep-ph/0104049](#)].

- [89] SHERPA collaboration, *Event generation with Sherpa 3*, *JHEP* **12** (2024) 156 [[2410.22148](#)].
- [90] F. Krauss, A. Price and M. Schönherr, *YFS Resummation for Future Lepton-Lepton Colliders in SHERPA*, *SciPost Phys.* **13** (2022) 026 [[2203.10948](#)].
- [91] A. Price and F. Krauss, *Towards a Fully Automated Differential NNLO_{EW} Generator for Lepton Colliders*, [2512.04959](#).
- [92] G. Balossini, C.M. Carloni Calame, G. Montagna, O. Nicrosini and F. Piccinini, *Matching perturbative and parton shower corrections to Bhabha process at flavour factories*, *Nucl. Phys. B* **758** (2006) 227 [[hep-ph/0607181](#)].
- [93] L. Flower and M. Schoenherr, *Photon splitting corrections to soft-photon resummation*, *JHEP* **03** (2023) 238 [[2210.07007](#)].
- [94] F. Jegerlehner, *Hadronic Contributions to Electroweak Parameter Shifts: A Detailed Analysis*, *Z. Phys. C* **32** (1986) 195.
- [95] H. Burkhardt, F. Jegerlehner, G. Penso and C. Verzegnassi, *Uncertainties in the Hadronic Contribution to the QED Vacuum Polarization*, *Z. Phys. C* **43** (1989) 497.
- [96] S. Eidelman and F. Jegerlehner, *Hadronic contributions to $g-2$ of the leptons and to the effective fine structure constant $\alpha(M(z)^{**2})$* , *Z. Phys. C* **67** (1995) 585 [[hep-ph/9502298](#)].
- [97] F. Jegerlehner, *The Role of $\sigma(e^+ e^- \rightarrow \text{hadrons})$ in precision tests of the standard model*, *Nucl. Phys. B Proc. Suppl.* **131** (2004) 213 [[hep-ph/0312372](#)].
- [98] F. Krauss, R. Kuhn and G. Soff, *AMEGIC++ 1.0: A Matrix element generator in C++*, *JHEP* **02** (2002) 044 [[hep-ph/0109036](#)].
- [99] T. Gleisberg and S. Hoeche, *Comix, a new matrix element generator*, *JHEP* **12** (2008) 039 [[0808.3674](#)].
- [100] B. Biedermann, S. Bräuer, A. Denner, M. Pellen, S. Schumann and J.M. Thompson, *Automation of NLO QCD and EW corrections with Sherpa and Recola*, *Eur. Phys. J. C* **77** (2017) 492 [[1704.05783](#)].
- [101] S. Kallweit, J.M. Lindert, S. Pozzorini, M. Schönherr and P. Maierhöfer, *NLO QCD+EW automation and precise predictions for V +multijet production*, in *50th Rencontres de Moriond on QCD and High Energy Interactions*, pp. 121–124, 5, 2015 [[1505.05704](#)].
- [102] S. Actis, A. Denner, L. Hofer, J.-N. Lang, A. Scharf and S. Uccirati, *RECOLA: REcursive Computation of One-Loop Amplitudes*, *Comput. Phys. Commun.* **214** (2017) 140 [[1605.01090](#)].
- [103] F. Buccioni, J.-N. Lang, J.M. Lindert, P. Maierhöfer, S. Pozzorini, H. Zhang et al., *OpenLoops 2*, *Eur. Phys. J. C* **79** (2019) 866 [[1907.13071](#)].
- [104] A. Denner, S. Dittmaier and L. Hofer, *Collier: a fortran-based Complex One-Loop Library in Extended Regularizations*, *Comput. Phys. Commun.* **212** (2017) 220 [[1604.06792](#)].
- [105] G. Ossola, C.G. Papadopoulos and R. Pittau, *CutTools: A Program implementing the OPP reduction method to compute one-loop amplitudes*, *JHEP* **03** (2008) 042 [[0711.3596](#)].
- [106] A. van Hameren, *OneLoop: For the evaluation of one-loop scalar functions*, *Comput. Phys. Commun.* **182** (2011) 2427 [[1007.4716](#)].

- [107] G. Abbiendi, E. Budassi, C.M. Carloni Calame, A. Gurgone and F. Piccinini, *Lepton pair production in muon-nucleus scattering*, *Phys. Lett. B* **854** (2024) 138720 [[2401.06077](#)].
- [108] E. Budassi, C.M. Carloni Calame, C.L. Del Pio and F. Piccinini, *Single π^0 production in μe scattering at MUonE*, *Phys. Lett. B* **829** (2022) 137138 [[2203.01639](#)].
- [109] C. Bierlich, A. Buckley, J.M. Butterworth, C. Gutschow, L. Lonnblad, T. Procter et al., *Robust independent validation of experiment and theory: Rivet version 4 release note*, *SciPost Phys. Codeb.* **36** (2024) 1 [[2404.15984](#)].
- [110] A. Buckley, J. Butterworth, D. Grellscheid, H. Hoeth, L. Lonnblad, J. Monk et al., *Rivet user manual*, *Comput. Phys. Commun.* **184** (2013) 2803 [[1003.0694](#)].
- [111] E. Spedicato, *Event reconstruction and analysis in the MUonE experiment*, Ph.D. thesis, Bologna U., 2025. [10.48676/unibo/amsdottorato/12202](#).
- [112] S. Jadach, B.F.L. Ward and Z. Was, *Coherent exclusive exponentiation for precision Monte Carlo calculations*, *Phys. Rev. D* **63** (2001) 113009 [[hep-ph/0006359](#)].
- [113] S. Jadach, B.F.L. Ward and Z. Was, *The Precision Monte Carlo event generator KK for two fermion final states in $e^+ e^-$ collisions*, *Comput. Phys. Commun.* **130** (2000) 260 [[hep-ph/9912214](#)].